Pairing morphology with gene expression in thyroid hormone-induced intestinal remodeling and identification of a core set of TH-induced genes across tadpole tissues

Daniel R. Buchholz [1], Rachel A. Heimeier, Biswajit Das, Teresa Washington, Yun-Bo Shi *

Section on Molecular Morphogenesis, Program on Cell Regulation and Metabolism, LGRD, NICHD, NIH, Building 18 T, Room 106, Bethesda, MD 20892-5431, USA

Abstract

Thyroid hormone (T3) plays a central role in vertebrate post-embryonic development, and amphibian metamorphosis provides a unique opportunity to examine T3-dependent developmental changes. To establish a molecular framework for understanding T3-induced morphological change, we identified a set of gene expression profiles controlled by T3 in the intestine via microarray analysis. Samples were obtained from premetamorphic *Xenopus laevis* tadpole intestines after 0, 1, 3, and 6 days of T3 treatment, which induces successive cell death and proliferation essential for intestinal remodeling. Using a set of 21,807 60-mer oligonucleotide probes representing >98% of the Unigene clusters, we found that 1997 genes were differentially regulated by 1.5-fold or more during this remodeling process and were clustered into four temporal expression profiles; transiently up- or downregulated and late up- or downregulated. Gene Ontology categories most significantly associated with these clusters were proteolysis, cell cycle, development and transcription, and electron transport and metabolism, respectively. These categories are common with those found for T3-regulated genes from brain, limb, and tail, although more than 70% of T3-regulated genes are tissue-specific, likely due to the fact that not all genes are annotated into GO categories and that GO categories common to different organs also contain genes regulated by T3 tissue specifically. Finally, a core set of upregulated genes, most previously unknown to be T3-regulated, were identified and enriched in genes involved in transcription and cell signaling.
© 2006 Elsevier Inc. All rights reserved.

Keywords: Frog metamorphosis; Thyroid hormone; Intestine remodeling; Microarray

Introduction

Amphibian metamorphosis, involving complete resorption, de novo development, and organ remodeling, is perhaps the most dramatic post-embryonic developmental event induced by a hormone (Shi, 1999; Tata, 1993). Even though most vertebrates lack metamorphosis, post-embryonic development is dependent upon the same hormones in all vertebrates studied. Intestinal remodeling at metamorphosis transforms the larval herbivorous intestine to the adult carnivorous gut via prodigious amounts of cell death and cell proliferation. During this time, larval cells are completely replaced by adult progenitor cells, source unknown, and the trough–villus axis with basal stem cells is established (Shi and Ishizuya-Oka, 1996). The molecular processes underlying how tissue can be remodeled, how cells interact with each other in development, and how gene expression is regulated are largely unknown in any vertebrate.

Soon after the nearly century-old discovery of the accelerating affect of the thyroid on frog metamorphosis, major advances in the endocrine and biochemical bases for this process have been elucidated (Dodd and Dodd, 1976; Shi, 1999; Tata, 1993). More recently, discovery of the role of the thyroid hormone (T3) receptor (TR) in gene regulation has allowed the beginning of a molecular description of the metamorphic

process. Now, with the advent of microarray technology with its power to profile gene expression changes globally throughout the genome, identification of the complete gene regulation cascade induced by T3 is within reach and can reveal for the first time the molecular players and associated cell and developmental pathways involved in this process. Initial progress in this direction has been to identify a handful of genes using subtractive hybridization in various hormone-induced tissues, such as limb, tail, intestine, and brain (Amano and Yoshizato, 1998; Buckbinder and Brown, 1992; Denver et al., 1997; Shi, 1999; Shi and Brown, 1993; Wang and Brown, 1993), followed by macroarrays to identify additional hormone-induced genes in the tail (Helbing et al., 2003). Genome-wide microarray data have been obtained from the brain, limb, and tail after a fixed period of hormone treatment (Das et al., 2006). In order to identify genes and developmental pathways important at different steps along the process of intestinal remodeling and to determine similarity in hormone-induced genes across tissues, we performed microarray experiments to identify temporal changes in gene expression at multiple time points during thyroid hormone-induced intestinal remodeling.

Materials and methods

Samples and hybridizations

Tadpoles of *Xenopus laevis* were reared in the laboratory or purchased from *Xenopus* 1, Inc. Premetamorphic tadpoles (stage 53) (Nieuwkoop and Faber, 1956) were treated with 10 nM triiodothyronine (T3) for 0, 1, 3, and 6 days at 18 °C with daily water changes and hormone replacement without feeding at a density of 5 tadpoles per liter. The anterior region of the intestine was isolated, flushed of contents, and snap frozen before isolation of total RNA using Trizol (Invitrogen). Three to five tadpoles were pooled for each of three biological replicates per treatment. High quality of total RNA was shown by capillary electrophoresis using a BioAnalyzer (Agilent). Cy3-CTP-labeled cRNA was prepared using Low RNA Input Linear Amplification Kit (Agilent). Reference mRNA from whole tadpoles at stages throughout metamorphosis (stages 50–66) was labeled with Cy5-CTP in advance and stored at −80 °C until needed (Das et al., 2006). A two-color reference design, where each RNA sample is hybridized with the reference sample, was used to make the data directly comparable between experiments. To minimize the technical variance among samples, all experimental samples were labeled and hybridized to the arrays at the same time according to the standard protocol using *X. laevis* whole genome Oligonucleotide Microarray, reference number AMADID 012454, according to manufacturer's instructions (Agilent).

Microarray data analysis

Hybridized slides were scanned using Agilent Scan Control software and Agilent Scanner G2505B (Agilent). The resulting signals of the 21,807 gene features per array were extracted from scanned microarray images using Feature Extraction 8.5 software (Agilent) using default settings in the FE protocol GE2_22k_1005 with local background subtraction and dye normalization. Data were subsequently processed using GeneSpring GX software (Agilent), which divides raw Cy3 fluorescence intensity values by the Cy5 control values and normalizes all spots on the array to the 50th percentile. Then, data were filtered to exclude saturated and/or non-uniform features or features not positive and significant above background. To identify significantly related genes, GeneSpring GX was further used to perform one-way ANOVA without assuming all variances were equal and setting Benjamini and Hochberg false discovery rate to $\alpha = 0.05$. Lists of significant genes were used for Gene Ontology mapping and pathway analysis in GeneSpring GX. GenMAPP and MAPPfinder were also used generate and validate significant molecular signaling pathways enriched in

the gene expression profiles (Dahlquist et al., 2002; Doniger et al., 2003). Most of the annotations of the genes were done using homologous genes in human.

Validation of array data using RT-PCR and RT-qPCR analysis

Total RNA was made into cDNA using High Capacity cDNA archive kit (Applied Biosystems) using the same RNA samples as in the microarray to confirm the microarray data. Additionally, intestinal cDNA was made from new samples of tadpoles treated under the same conditions to establish the universality of the microarray results. Forward and reverse primers were designed on separate exons based on sequences from indicated GenBank accessions and the *Xenopus tropicalis* genome to avoid amplification of contaminating genomic DNA (Supplementary Table S1). Quantitative PCR was carried out using primers and FAM-labeled TaqMan probes (Applied Biosystems) (Supplementary Table S2) with cDNA standards made from whole body total RNA from tadpoles at stages 50–66.
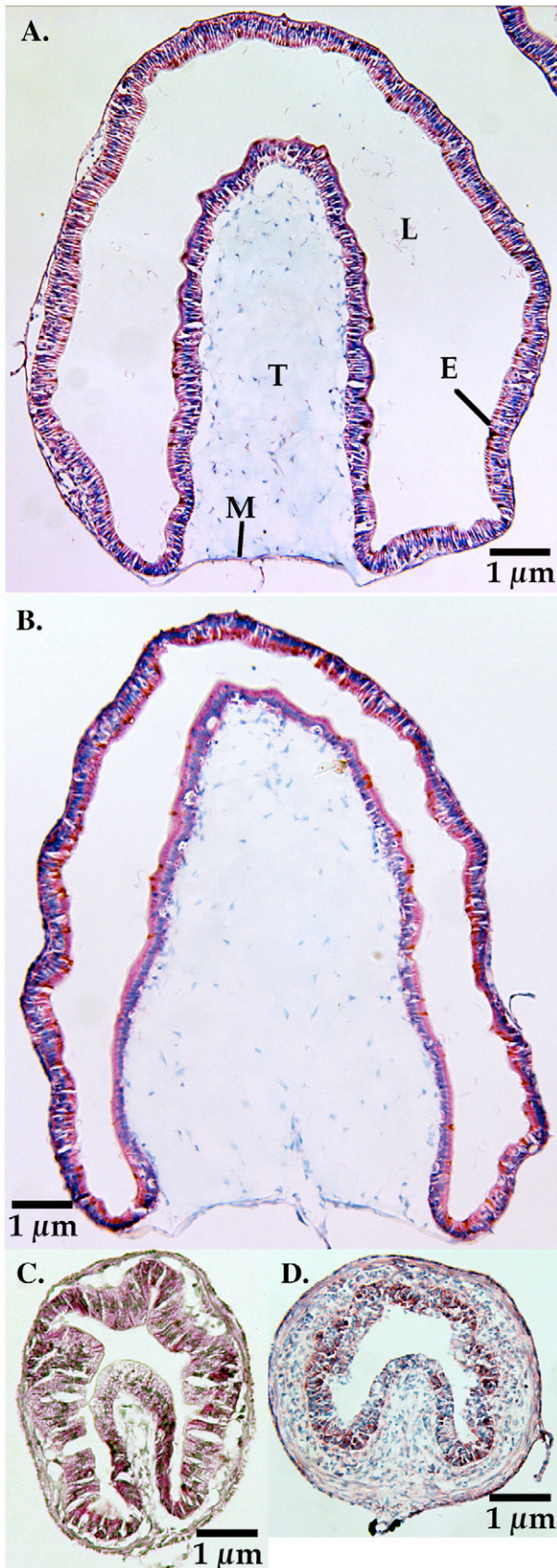
Histology

To determine the phenotypic change in the intestine for each treatment group, methyl green pyronine Y staining on intestine sections was performed as described previously (Buchholz et al., 2004).

Results

Morphological assessment of T3-induced intestine development

A major goal of microarray experiments is to provide a gene expression profile that correlates with phenotypic change. To obtain an overview of the gene regulation cascade triggered by the T3 during intestinal remodeling, this study used a two-color reference design to identify differentially regulated genes between total RNA samples from control versus T3-treated tadpoles in which intestinal remodeling has been induced. T3 treatments of premetamorphic tadpoles (10 nM T3 for 1, 3, and 6 days at 18 °C) resulted in well-established morphological changes, such as gill resorption, limb outgrowth, head shape remodeling, and intestinal shortening (data not shown) (Dodd and Dodd, 1976; Shi, 1999). Histological examination of the T3-treated intestine revealed the well-known tissue remodeling response to T3 (Fig. 1) (Shi and Ishizuya-Oka, 1996). Untreated intestinal cross-sections were characterized by thin muscle around the outside, a simple epithelium, and a single in folding, the typhlosole, which contains the majority of connective tissue in the larval intestine. Little morphological change occurred after 1 day of hormone treatment, but by 3 days, the muscle and connective tissue layers increased in thickness. Larval epithelial degeneration was evident, in agreement with previous studies showing the high proportion of apoptotic larval epithelial cells at this time (Ishizuya-Oka and Ueda, 1996; Ishizuya-Oka et al., 1997b; Shi and Ishizuya-Oka, 1996). By Day 6, the T3-induced changes in the muscle and connective tissue have become more pronounced, and most of the larval epithelium has undergone cell death, while proliferating adult cells appear (Fig. 1). Thus, histological analysis on the intestine samples from each treatment group showed that the collected RNA samples should represent specific progress time points during the remodeling process, i.e., from the initial induction of larval epithelial cell death (Day 1), to active cell death (Day 3), and the near

completion of cell death and the early stages of adult epithelial cell proliferation (Day 6). Therefore, microarray analysis of the RNA samples should provide molecular profiles of gene expression associated with each of these developmental phases in the remodeling intestine.

Quality control and statistical analyses

For each treatment group (0, 1, 3, and 6 days of T3 treatment), we used three biological replicates, each consisting of 3–5 pooled intestines. After labeling, hybridizing, and scanning all samples simultaneously, a number of quality control analyses were performed to filter the resulting expression level data before identifying genes significantly regulated by T3. Initial quality control of the data, involving image analysis, background correction, and normalization of the 21,807 spots on the array, revealed high quality data for 14,331 genes, whose features were uniform, not saturated, and significantly above the local background signal, and these criteria were met on at least two of the twelve hybridized arrays. At the sample level, we examined box plots to ensure that the normalization procedure properly centered the fluorescence intensity distribution at 1 (the 50th percentile of all spots on the chip) and that the spread of these distributions was similar across all samples (Fig. 2A). Finally, analysis of the normalized log intensity values across all high quality features on the array revealed, as expected, that replicates within treatments clustered with each other (Fig. 2B). Furthermore, treatments clustered according to T3 treatment, where increased T3 treatment duration reduced the similarity between treated and untreated samples.

To identify significantly regulated genes, we performed ANOVA across all treatments and used a false discovery rate (FDR) set to $\alpha = 0.05$. We found 2340 significantly regulated genes, and 1997 of these had a fold change greater than 1.5 between Day 0 and Days 1, 3, and/or 6 (Supplementary Table S3). The number of significantly regulated genes increased with days of T3 treatment (Fig. 3), and in total, 1211 genes were upregulated on at least one time point, and 903 genes were downregulated (Fig. 3). A number of genes, 117, were both up-

Fig. 1. Effects of T3 on intestine histology. Tadpoles were treated with 10 nM T3 for 0, 1, 3, or 6 days at 18 °C. Intestine was isolated, sectioned and stained with methyl green pyronine Y. (A) Intestine cross-sections of untreated tadpoles (Day 0) show a lumen (L) surrounded by columnar layer of epithelium (E) with a single in folding, the typhlosole (T), composed of connective tissue, which is thin elsewhere. The thin outer layer is muscle (M). The cytoplasm of the epithelial cells was uniformly stained red by the pyronine Y, which binds strongly to RNA. (B) Very little morphological change occurred after 1 day of hormone treatment. (C)After 3 days of treatment, the muscle began to thicken and connective tissue appeared much more prominent in between the muscle and epithelial layers. Larval epithelial degeneration was evident by reduction of pyronine Y staining in many areas and folding due to contraction. (D) After 6 days of T3 treatment, the changes in the muscle and connective tissue are more pronounced. Most of the larval epithelial cells had undergone apoptosis and the variation in epithelial staining intensity was reflective of epithelial replacement, with the remaining larval epithelial cells facing the lumen poorly stained with the red pyronine Y while the proliferating adult epithelial precursors close to the connective tissue were strongly stained.
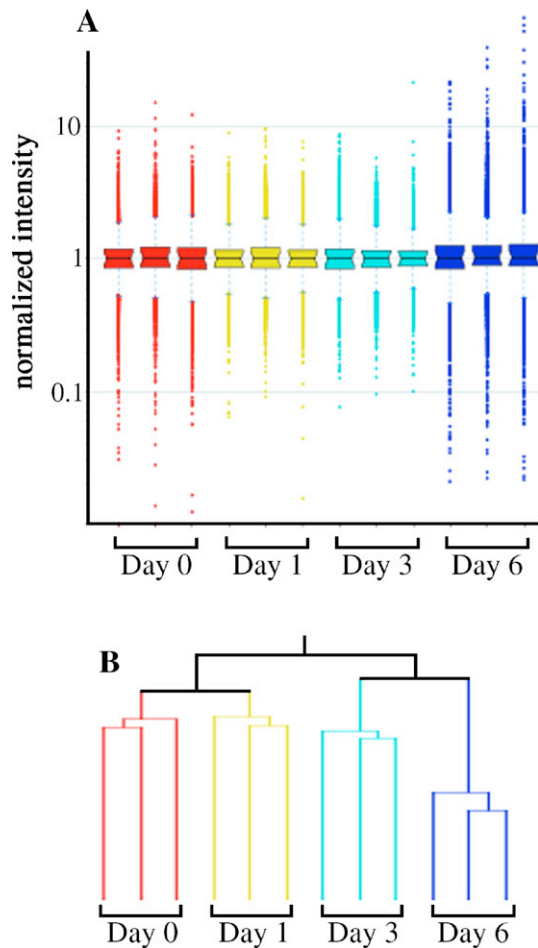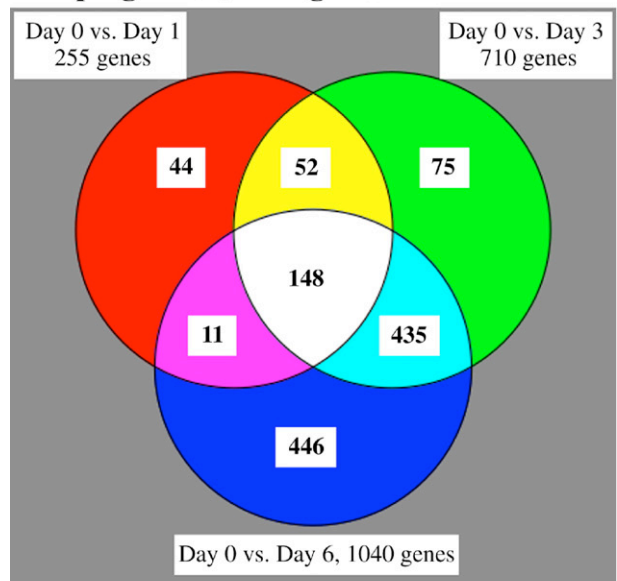
Fig. 2. Quality control analyses on the microarray samples. (A) The box plots of each replicate used in the experiment show proper centering of the samples normalized to a fluorescence intensity of one (the 50th percentile of all spots on each chip). Each sample has a similar distribution of normalized spot intensities as indicated by the similar sized boxes, which represent expression levels for 50% of the genes. The dashed lines encompass 37% of the genes whose normalized intensity values lie above or below the boxes, and the points represent individual genes (the remaining 13%) with outlying normalized intensity values. (B) The dendrogram of each sample grouped by similarity of expression levels across all high quality spots on the array shows that replicate samples within each treatment are most similar to each other and that Day 3 and Day 6 treatments are more similar to each other than to Day 0 and Day 1 treatments.

and downregulated, but on different days. There were 148 upregulated genes common to all three treatments (1, 3, 6 days) and 86 common downregulated genes. The highest number of shared regulated genes was between Day 3 and Day 6, whereas Day 1 and Day 6 shared the least number of regulated genes. These data indicate that hormone-induced changes in gene expression correlate with progressive morphological change.

Gene list verification

Even though microarray protocols are now well established, it is nevertheless important to independently evaluate the quality of the microarray data because false positives and false negatives do exist. We verified the microarray data quality in three ways. First, we examined expression levels of four
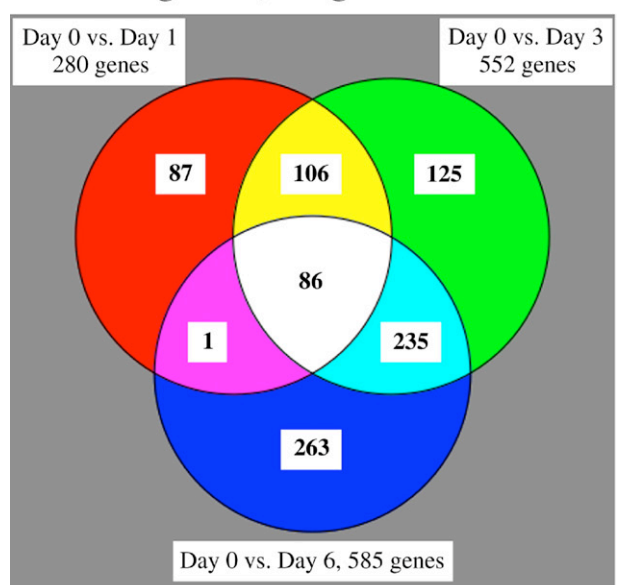

Fig. 3. Venn diagrams showing numbers of genes up- and downregulated. (A) A total of 1211 genes were upregulated in response to T3. The number of these genes upregulated at Days 1, 3, and 6 in comparison to Day 0 is indicated under the specific comparison, and number of genes upregulated by T3 increases with duration of hormone treatment. There were 148 genes upregulated at all three time points, and 44, 75, and 446 genes were upregulated only on Days 1, 3, and 6, respectively. Between 11 and 435 genes were upregulated on only two of the three time points. Lists of upregulated and downregulated genes on Day 1, 3, and 6 are in Supplemental Tables S3. (B) A total of 903 genes were downregulated in response to T3. The number of these genes downregulated at Days 1, 3, and 6 in comparison to Day 0 is indicated under the specific comparison, and number of genes downregulated by T3 increases only between Days 1 and 3, not Day 6. There were 86 genes downregulated at all three time points, and 87, 125, and 263 genes were downregulated on only Day 1, 3, and 6, respectively. Between 1 and 263 genes were downregulated on only two of the three time points.

previously known T3 response genes by comparing microarray data with results from reverse transcriptase (RT) followed by quantitative PCR (qPCR) using the TaqMan method (Fig. 4). Thyroid hormone receptor beta is a direct response gene induced by T3 in all tissues of the intestine (Ranjan et al., 1994; Shi and Ishizuya-Oka, 1997). Stromelysin-3 and sonic hedge-

hog are also direct response genes whose induction by T3 in the intestine is restricted to the fibroblasts and epithelial cells, respectively (Patterton et al., 1995; Stolow and Shi, 1995). Intestinal fatty acid binding protein (IFABP) is a down-regulated, late response gene of the intestinal epithelium (Shi and Hayes, 1994). Because the same total RNA samples were
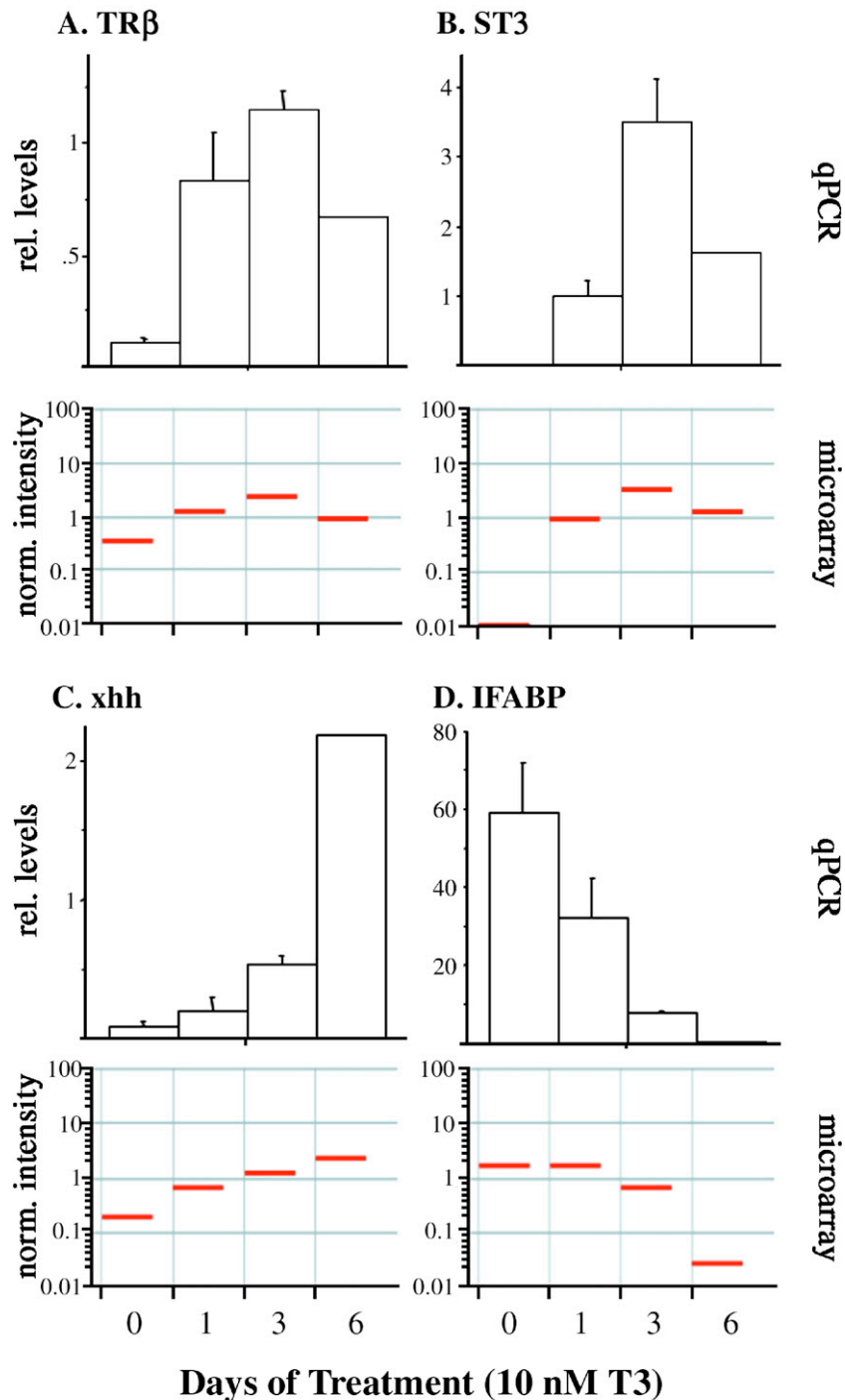

Fig. 4. Quantitative RT-PCR verification of known T3 response genes. cDNA was made from total RNA used in the microarray, and quantitative PCR was used to detect (A) thyroid hormone receptor beta (TRβ), (B) stromelysin-3 (ST3), (C) sonic hedgehog (xhh), and (D) intestinal fatty acid binding protein (IFABP). The expected increase in relative levels of transcript with respect to the control gene ribosomal protein L8 (not shown) was observed in panels A–C and the expected decrease in panel D. The lower portion of each panel shows the normalized intensity from the microarray analysis for each gene. Note the rank order differences between RT-qPCR and microarray correspond exactly.

used in the RT-qPCR and microarray, the similar pattern of regulation for all four genes in both the microarray and RT-qPCR shows the ability of the microarray to reflect gene expression levels. The range of raw fluorescence intensity values for these four genes varied from 300–2215 in TRβ to 13,894–817,634 in IFABP, indicating that the microarray is sensitive and accurate to both low copy and high copy messages.

We also compared our microarray data with previously obtained subtractive hybridization data performed on the intestine (Shi and Brown, 1993). In that study, 22 upregulated genes were identified after an 18-h treatment with 5 nM T3 at room temperature, and, of those, 12 were represented on the microarray (Table 1). Six of these regulated genes were confirmed by the microarray data, and five had undetectable expression levels for the microarray. There was a single discrepancy, Na/PO_4 cotransporter, where the subtractive hybridization data showed T3 regulation (Ishizuya-Oka et al., 1997a; Shi and Brown, 1993) and the microarray showed non-significant gene expression change in response to T3 in any of the treatments, though the explanation for this discrepancy is not clear.

Finally, we verified differential expression of some genes previously unknown to be regulated by T3 using RT-PCR. Five upregulated genes and five downregulated genes were chosen that were at least 2.5-fold regulated across all days of treatment so their putative regulation could be detected by RT-PCR assay. In addition, we used total RNA isolated independently from that used in the microarray to assess the generality of the microarray data. All selected genes were confirmed by RT-PCR to be regulated as indicted by the microarray data (Fig. 5). In addition, four other genes downregulated by at least 2.5-fold on fewer than all 3 treatment days were tested and showed that three of the four were confirmed using independently isolated RNA (data not shown).

Table 1
Comparison of data from subtractive hybridization and microarray experiments

Gene ID	Gene name	Microarray	GenBank
TRβ	TRβ	S	M35362
Tail 8	TH/bZIP	ND	U37375
Tail 9	TH/bZIP	ND	U41859
Tail 14	Stromelysin-3	S	Z27093
IU1/IU12	TH transporter	S	BC060751
IU3	CEACAM8	ND	CF548522
IU20	Spermine oxidase	ND	BU900580
IU21	Novel gene	ND	BJ051621
IU22	Non-hepatic arginase	S	U08407
IU23	Sulfotransferase, cytosolic 1	S	CB561452
IU24	Na/PO_4 cotransporter	NS	BG264222
IU27	Sonic hedgehog	S	L39213

All 12 genes (Gene ID) identified by a subtractive hybridization experiment (Shi and Brown, 1993) that were present on the microarray are listed. The subtractive hybridization screen isolated only upregulated genes. S=significant on array, ND=not detected on array, NS=not significant on array.

Note. Twenty-two genes were initially isolated in the subtractive hybridization screen. Twelve of these genes were represented on the array and shown above. The ten remaining were either not sequenced (*IU30, IU34*), were duplicates (*IU1/IU12, IU10/IU19*), lacked homology with a known gene (*IU9, IU14*), or were absent in UniGene Build 48, the basis of this array design (*IU5, IU16, IU33, IU10/IU19*).

A. Up-regulated Genes

amyloid precursor protein secretase (BC046667)

HMG-box containing protein 1 (AF530514)

histadine ammonia lyase (BE507589)

kidney est., 5' read (CF547202)

inhibitor of DNA binding 4 (BC045022)

rpL8

B. Down-regulated Genes

methionine adenosyltransferase II (BC043970)

hyp. protein MGC53111 (BC046688)

cationic amino acid transporter (BC044971)

5,10-methylenetetrahyrofolate reductase (NADPH) (BC046708)
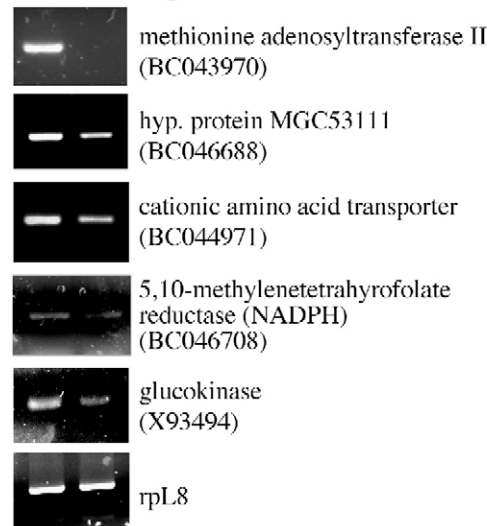
glucokinase (X93494)

rpL8

Fig. 5. Verification of T3-regulated genes newly identified by the microarray. Primer pairs to PCR amplify ten genes regulated across all days of treatment with a fold change of greater than 2.5 based on the array were designed and used on cDNA made from independently isolated total RNA from Day 0 and Day 1 intestines. (A) All five upregulated genes and (B) all five downregulated genes tested by RT-PCR showed the same regulation pattern as identified by the microarray. GenBank accession numbers are shown under gene names, and *rpL8* (ribosomal protein L8) is a control gene, unregulated by T3.

Global expression profile analysis and associated biological functions

Because the time course of gene expression may give clues to its developmental significance, we clustered genes based on temporal expression profiles and then determined whether these clusters may be associated with distinct biological functions. First, we analyzed the 2340 statistically significant genes by a *K*-means nonhierarchical clustering method using GeneSpring, which uses normalized intensity and temporal expression pattern to cluster genes. With this method, we identified four predominant clusters: (1) increased transiently (287 genes), (2)
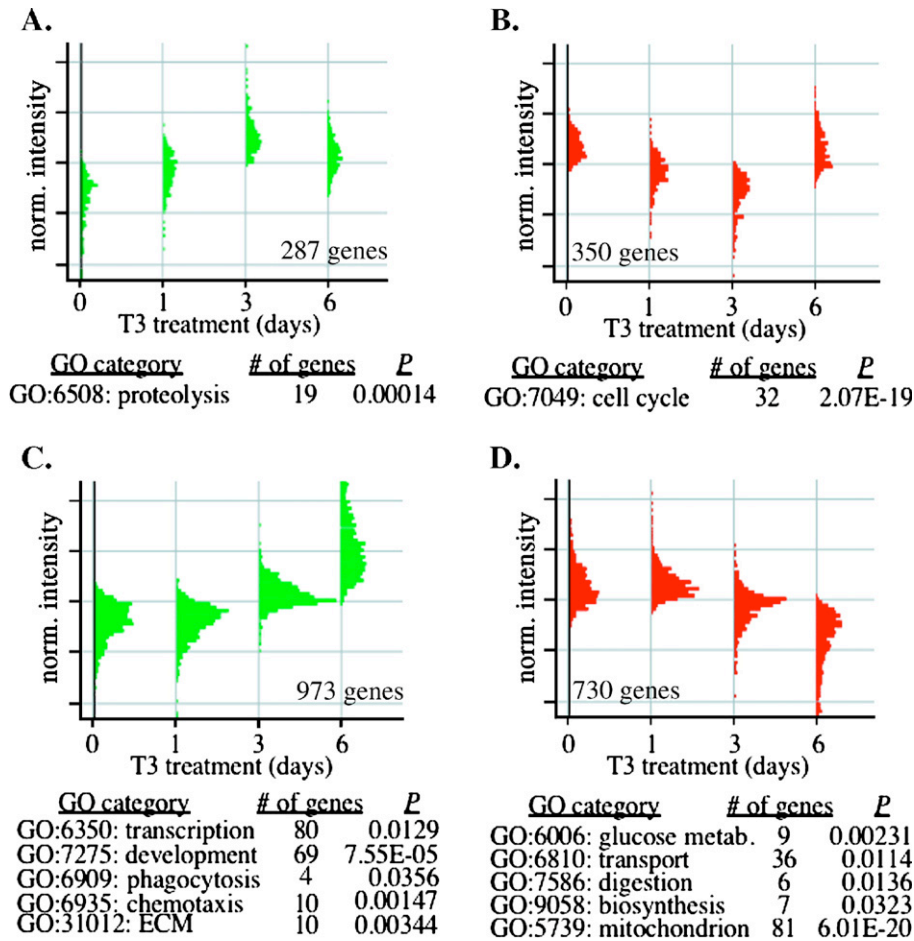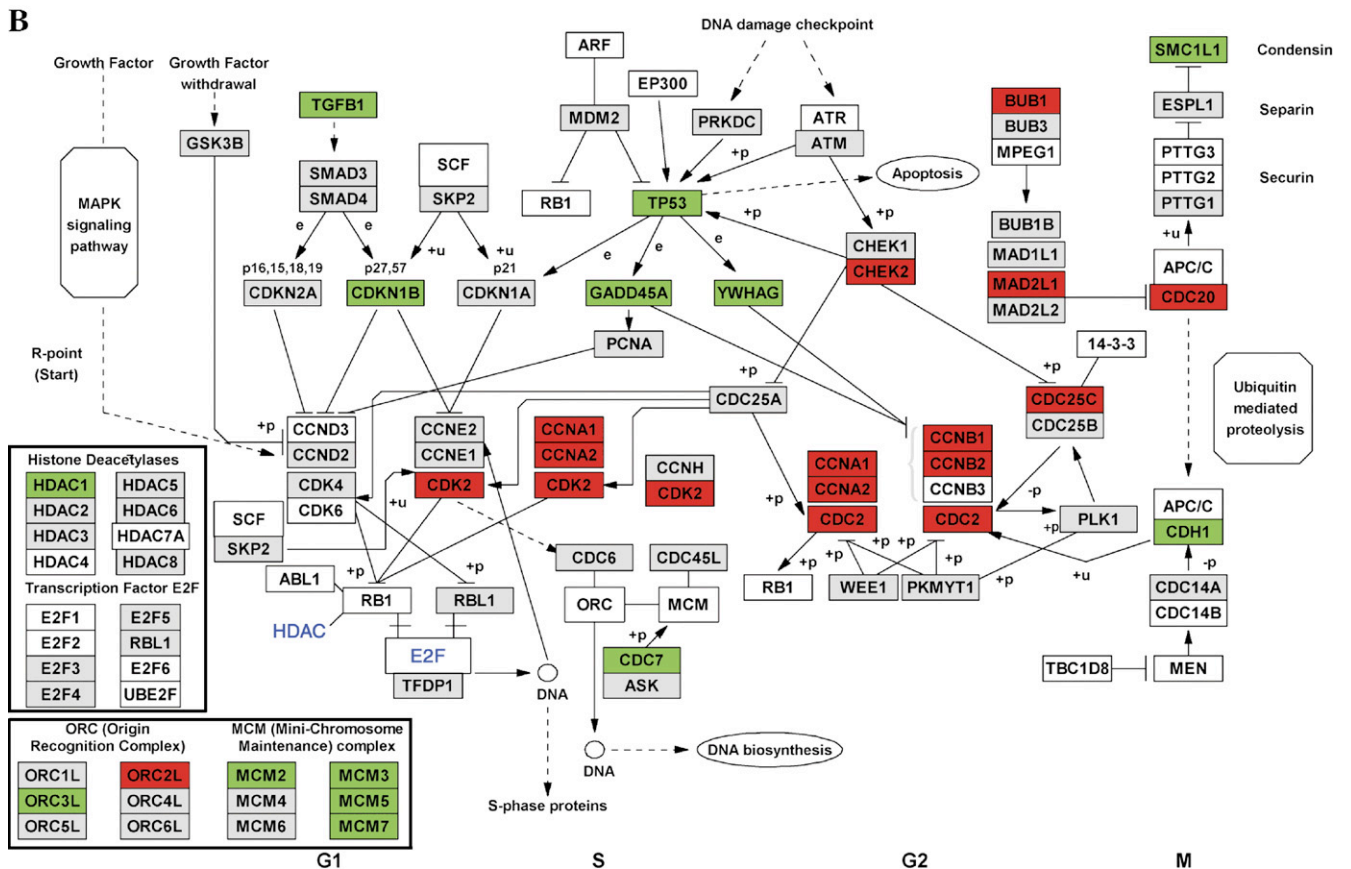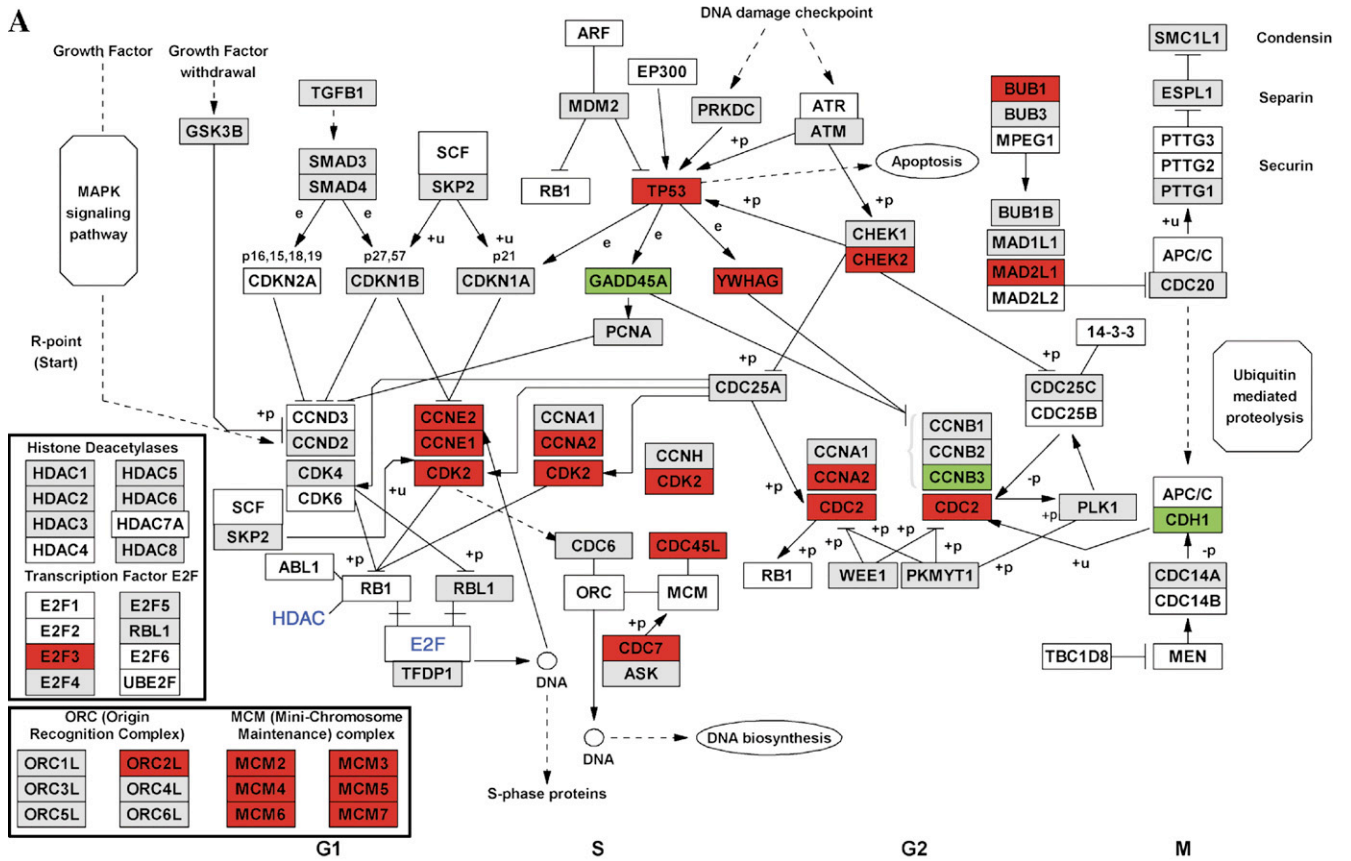
Fig. 6. Gene clusters based on temporal patterns of expression and associated gene ontology (GO) categories. *K*-means clustering analysis revealed four temporal patterns of regulated gene expression, (A) transiently upregulated, (B) transiently downregulated, (C) upregulated late, and (D) downregulated late. The number of genes in each cluster is indicated in the graphs. Below each graph, significant and non-redundant GO categories for each gene cluster are listed, as well as the number of genes from the cluster in the category and associated *p*-values. The genes represented in this figure are listed in Supplemental Table S4.

decreased transiently (350 genes), (3) late upregulated (973 genes), or (4) late downregulated (730 genes) (Fig. 6). Because *K*-means clustering uses both normalized intensity and expression pattern instead of just fold change relative to Day 0, most genes will follow the average pattern for the cluster, but not all. For example, the late upregulated cluster may include genes that are continuously increasing beginning on Day 1.

With these four identified temporal expression clusters, we used the Gene Ontology (GO) database to identify the biological functional categories that are statistically significantly enriched in these clusters of genes (Zeeberg et al., 2003). In addition to GO mapping, we used pathway analysis to associate potentially significant biological pathways from GenMAPP with gene lists. Different significant, non-redundant GO categories are associated with each gene expression cluster (Fig. 6). Because GO

annotation for *Xenopus* genes depends on Unigene homology with human proteins, only about half of the *Xenopus* genes on our array are annotated for GO categories. The first wave of 287 induced genes peaked after 3 days, for which the proteolysis GO category was significant and correlated with the apoptosis phase of intestinal remodeling (Fig. 6A). Our microarray data corroborated known genes associated with apoptosis and tissue breakdown, such as stromelysin-3 (**Z27903**) in larval apoptosis (Fu et al., 2005; Ishizuya-Oka et al., 2000; Patterton et al., 1995) and collagenase 3 (**U41824**) in tissue breakdown (Berry et al., 1998a,b; Damjanovski et al., 1999; Stolow et al., 1996), and extended this list to 19 induced genes in proteolysis GO category. These additional genes include cysteine and aspartyl proteases (**BC056842**, **BC056059**, **BC061685**) and peptidases (**CF522422**, **BC056069**, **BU901375**). A number of proteolysis

Fig. 7. Correlation of the regulation of genes in cell cycle pathway with tissue transformation. Genes significantly regulated by 1.5-fold on (A) Day 1 and (B) Day 6 were mapped onto the GenMAPP pathway for the cell cycle. Red boxes indicate gene downregulation on that day of treatment, and green boxes indicate upregulation. The regulation pattern of these genes falls predominantly into the transiently downregulated cluster, i.e., Day 1 and Day 3, correlating with TH induction of larval epithelial apoptosis. However, by Day 6 when adult cell proliferation is just beginning and larval cell death is near completion, much of the cell cycle downregulation is over and more genes are upregulated. The T3 response genes of the cell cycle that are downregulated in the intestine are the same genes upregulated in the brain and limb (see Discussion).

genes were represented in the late upregulated cluster, including *MMP1* (**BC054233**), *MMP2* (**BC054947**), and *gelatinase B* (**AF072455**), but because the overall number of genes in that cluster was larger, the proteolysis category was not significant in the late upregulated cluster. Simultaneous with cell death and initial remodeling, a wave of 350 downregulated genes included significant association with cell cycle progression genes, notably the minichromosome maintenance complex proteins MCM2-7, cyclin E3 (**L43513**), and cyclin-dependent kinase 2 (**X14227**) (Fig. 6B).
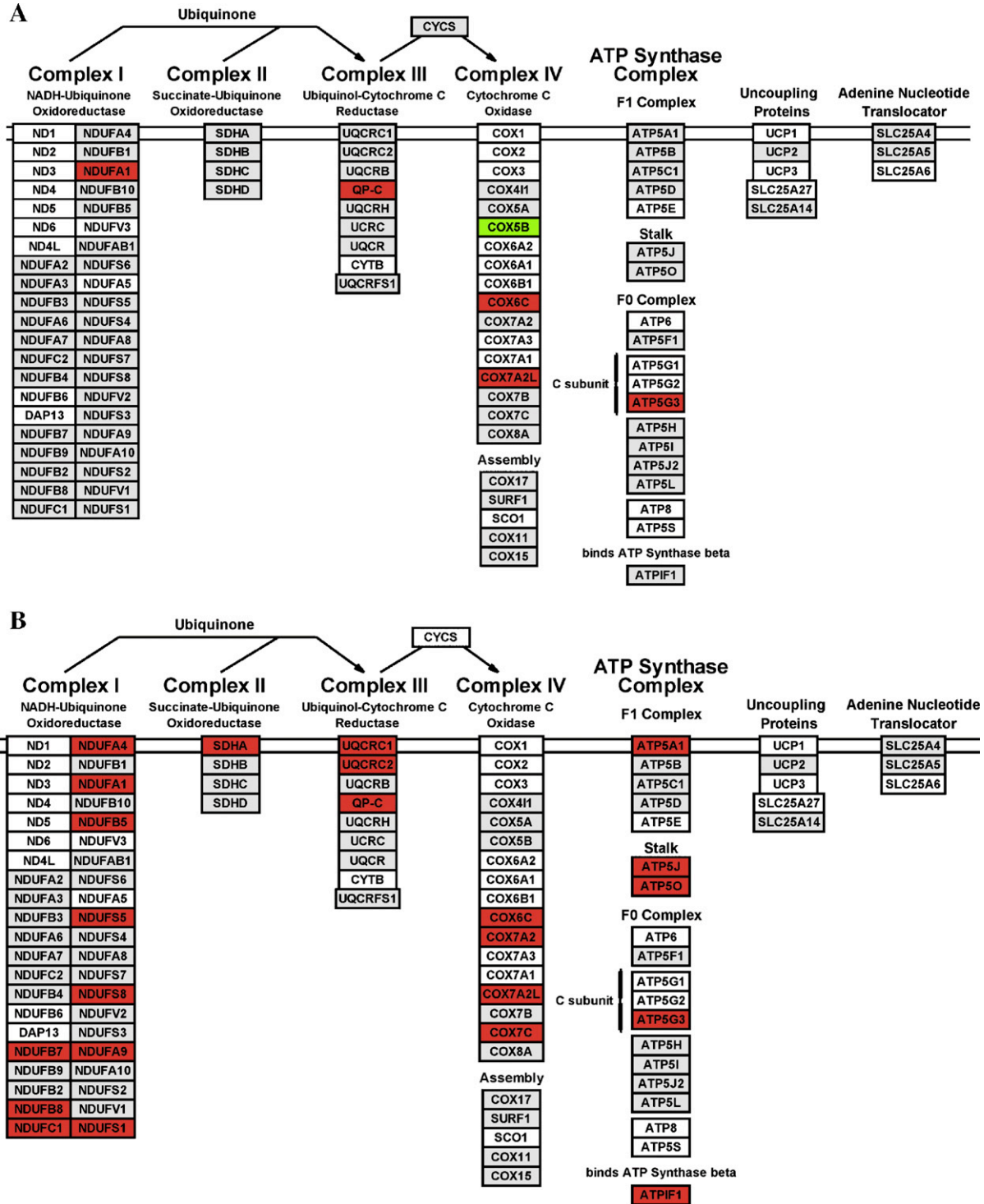

Fig. 8. Late downregulation of genes involved in electron transport correlates with cell death. Genes significantly regulated by 1.5-fold on (A) Day 1 and (B) Day 3 were mapped onto the GenMAPP pathway for electron transport. Red boxes indicate gene downregulation on that day of treatment, and green boxes indicate upregulation. The regulation pattern of these genes falls predominantly into the late downregulated cluster. Electron transport pathway is involved in energy metabolism, and this pathway and the glucose metabolism pathway are downregulated at the time when apoptosis is predominant and few adult cells are proliferating. The downregulation of these genes is likely due to late events during apoptosis and thus remains prominent even after 6 days when cell death is near completion.

Corroborating the GO categories was the identification of GenMAPP pathways significantly associated with the transiently changing genes. In the transiently downregulated cluster, the DNA replication pathway was significant ($p < 5.29e-18$), including the key regulators CDK2 (**X14227**) and Cdc45 (**AF062494**), and, as in GO mapping, the cell cycle was significantly downregulated ($p < 1.54e-28$) (Fig. 7). Mapping the fold change differences between Day 0 and the other treatment days for the cell cycle pathway revealed that 20 out of 30 downregulated genes were on Day 1 (Fig. 7A) and 24 of 30 on Day 3 (not shown), but only 12 of 30 were downregulated by Day 6 (Fig. 7B). In addition, 3 out of 14 upregulated genes for the cell cycle pathway were observed on Day 1 (Fig. 7A) and 4 out of 14 on Day 3 (not shown), while 13 out of 14 genes were upregulated by Day 6 (Fig. 7B).

Following the initial wave of gene expression change, the two other clusters of genes were regulated, either up or down after the initial wave. Here, the cluster whose 973 genes continued to increase in expression level during the treatments had significant GO categories, including transcription, development, and extracellular matrix (Fig. 6C). This group of genes is likely responsible for the second major transition of intestinal remodeling where small nests of proliferating cells make cell fate decisions and differentiate. For example, genes previously known to be involved in frog intestinal remodeling, such as sonic hedgehog (xhh, **L39213**) and bone morphogenic protein 4 (BMP-4, **X63426**), are in this temporal gene expression cluster. By virtue of pathway analysis, many additional genes associated with hedgehog signaling are coordinately regulated, such as patched 2 (**BJ029994**), hedgehog interacting protein (aka gene 5, **BC046952**), Gli 2 (**AF109923**), and Gli 3 (**U42461**). Similarly, the microarray data lend additional support to the importance of the transforming growth factor beta signaling pathway in intestinal remodeling by implicating multiple genes downstream of BMP-4 ($p < 0.0071$) (Supplemental Fig. S1). Interestingly, multiple members of the BMP family are upregulated, such as BMP-1, -2, -3, and -7 (**D83476**, **X63424**, **AB059563**, **BC055959**) and BMP type II receptor (**U81958**).

The remaining cluster has genes that are downregulated throughout the hormone treatments (Fig. 6D) and includes the significant GO clusters of glucose metabolism, transport, digestion, and genes located in the mitochondrion. Pathways significantly associated with this cluster were fatty acid beta-oxidation ($p < 1.12e-5$) and electron transport chain ($p < 3.39e-18$) (Fig. 8). These biological functions and pathways have not previously been associated with a particular histological event.

Meta-analysis: comparison with expression profiles of various tadpole tissues

Microarray data from other T3-responsive tissues, tail, limb, and brain (Das et al., 2006), of premetamorphic tadpoles treated with T3 for one fixed dose and time period are available to perform a meta-analysis in order to examine the basis for tissue-specific morphological response to T3 and to iden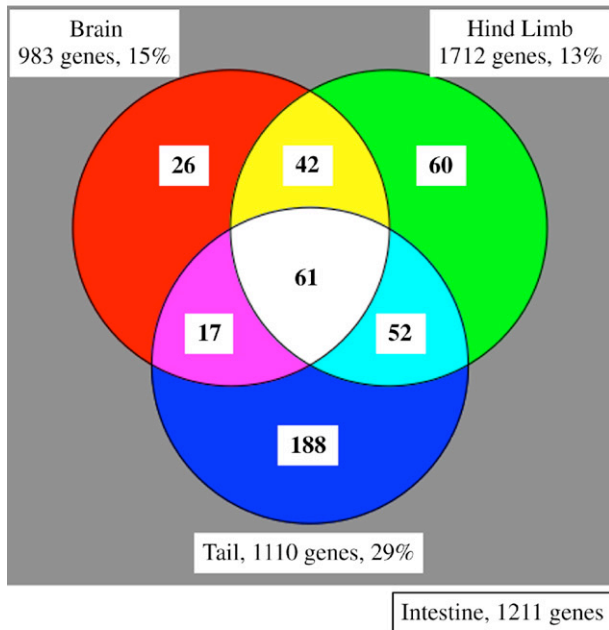tify, if any, a common set of core genes regulated by T3 in all tissues. Similar to the intestine, the brain remodels during metamorphosis, whereas the tail resorbs completely and the limbs develop de novo. All identified T3-respone genes from brain, hind limb, and tail (significantly regulated by 1.5-fold after 48 h of 100 nM T3 treatment at room temperature) (Das et al., 2006), were compared with all significantly regulated genes 1.5-fold in the intestine after 1, 3, and/or 6 days of T3 treatment (Fig. 9). Even though the treatment conditions were different, we used all identified genes from all four organs to gain as much overlap as possible among tissues. For the brain and hind limb, less than 15% of the genes were common with the intestine genes, either up- or downregulated, whereas the overlap of genes regulated in both tail and intestine was higher, 29% and 22% up- and downregulated, respectively. The number of genes identified that are upregulated in all tissues by T3 is 61 genes, where the majority of these genes fell into the categories of transcription factors followed by cell signaling, protein metabolism, and cell structure (Table 2). On the other hand, only three genes were downregulated in common among all tissues, FK 506-binding protein precursor (**CB198247**), pyruvate dehydrogenase kinase (**BC059972**), and sulfotransferase 1C1 (**AW645021**).

Discussion

Intestinal remodeling during metamorphosis involves well-established biological processes, such as apoptosis and tissue breakdown of larval epithelial cells, proliferation of connective tissue and muscle cells, and proliferation and differentiation of adult epithelial cells involving cell–cell interaction (Shi and Ishizuya-Oka, 1996). Our hormone treatments were chosen to focus on the initial steps of hormone-induced remodeling, and we were successful in capturing the processes of cell death and appearance of adult proliferative precursors. The histology suggests that Day 3 is the peak of apoptosis with some connective tissue and muscle proliferation. By Day 6, apoptotic larval cells are still present, but adult cell proliferation has begun, as well as continued muscle and connective tissue proliferation. Adult cell differentiation has not yet begun as evidenced by the lack of a return in the expression of IFABP, a marker for fully differentiated intestinal epithelial cells (Ishizuya-Oka et al., 1997b; Shi and Hayes, 1994). This temporal progress through the remodeling process allowed us to target-specific phases, namely initial gene induction on Day 1, and gave us the opportunity to completely separate the molecular events controlling induction of cell death from events controlling adult cell proliferation. A stronger hormone induction regimen would have resulted in contemporaneous expression of genes controlling larval cell death and adult cell differentiation.

Clustering of genes based on temporal expression after T3 treatments of 0, 1, 3, and 6 days (using *K*-means clustering) revealed four groups of genes whose expression profiles were significantly different from each other but the expression of genes within each cluster was similar to each other. Such temporal gene expression clusters may be associated with distinct biological functions associated with the morphological events occurring at the time. Indeed, by mapping these gene
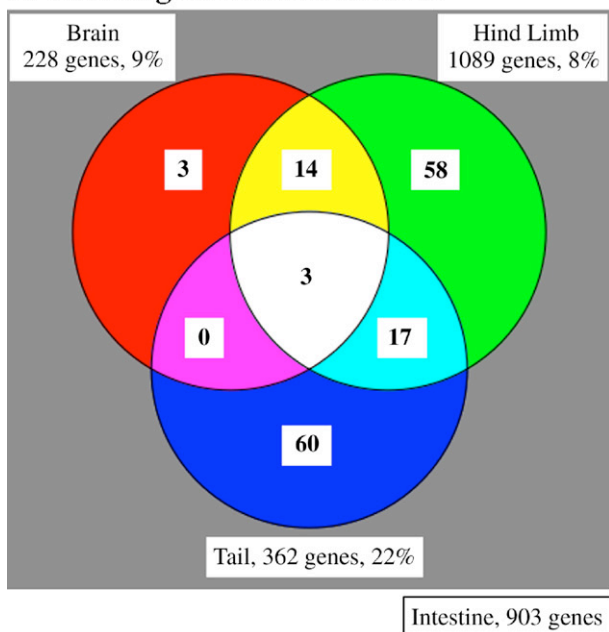
Fig. 9. Comparison of genes regulated by T3 across brain, hind limb, tail, and intestine. The number of genes upregulated (A) or downregulated (B) after 2 days of 100 nM T3 in brain, hind limb, and tail are indicated in the white boxes (Das et al., 2006). The total number of T3-regulated genes in the intestine identified in the current report is listed below the panels and is used for this comparison. The numbers listed in the Venn diagram are genes upregulated or downregulated in common between the intestine and the indicated tissue. For example, 26 genes are induced in both brain and intestine only, and 42 genes are induced in brain, hind limb, and intestine. The percentages represent the proportion of genes induced in the intestine that are also induced in the associated organ. Note that more upregulated genes are shared among organs than downregulated genes and that the tail shares more regulated genes with the intestine than the other organs. The core set of upregulated genes in all four tissues is listed in Table 2.

lists to Gene Ontology (GO) hierarchy and GenMAPP, the functions of genes within these clusters correlated in time with observed histological events induced by T3. Previously, several genes have been associated with these histological events, such as, stromelysin-3 in apoptosis (Fu et al., 2005; Ishizuya-Oka et al., 2000; Patterton et al., 1995) and sonic hedgehog and BMP-4 in adult epithelial cell development (Ishizuya-Oka et al., 2001a, b; Stolow and Shi, 1995). The microarray data greatly extended the correlation of gene expression with morphological change. The transiently up- and downregulated genes are strongly correlated with larval epithelial degeneration, which is the most significant early event in TH-induced remodeling (Ishizuya-Oka and Shimozawa, 1991; Ishizuya-Oka and Ueda, 1996; McAvoy and Dixon, 1977). The upregulated proteolytic genes, in addition to stromelysin-3, may help cause apoptosis by disruption of the extracellular matrix that is needed for epithelial cell survival. It is interesting that the significant GO categories do not include GO category for cell death/survival genes, even though cell death is a predominant early effect of T3 treatment. This is likely because many such genes such as *caspase* and *bcl-2* family genes may not change their mRNA levels significantly during metamorphosis and are regulated instead at the post-transcriptional level (Cruz-Reyes and Tata, 1995; Nakajima et al., 2000; Pasquier et al., 2006; Rowe et al., 2005; Sachs et al., 2004; Yaoita and Nakajima, 1997). In addition, the GO category includes both cell death promoting and cell death inhibiting genes, making it less likely to be a significant GO category in our array analysis. This is because significance in this analysis is based on whether the percentage of the genes in the category found to be regulated by the hormone (cell death promoting genes) is above the average expected for all genes in the category (both cell death inhibiting and promoting genes).

The transient downregulated genes involved with the cell cycle and DNA replication are likely a consequence of apoptotic signals in the degenerating larval epithelium. In addition, several transcription factors were transiently induced, such as Sox 4 (**BC059296**), Sox 7 (**D83649**), Kruppel-like factor 13 (**BX844667**), zinc finger protein 239 (**BE507064**), HMG-box transcription factor 1 (**AF530514**), and basic transcription element-binding protein 1 (**U35408**), and these likely represent an initial wave of transcription factors in the TH-induced gene regulation cascade. Taken together, these data suggest that changes in transient increase in expression of genes, including genes involved with proteolysis and cell cycle, underlie the morphology of apoptosis at 3 days and prepare the tissue for the dramatic events that are to come.

After the initial wave of apoptosis, adult cells proliferate and differentiate, accompanied by the proliferation of connective tissue and likely muscle cells (Ishizuya-Oka and Shimozawa, 1991; Ishizuya-Oka and Ueda, 1996; McAvoy and Dixon, 1977; Schreiber et al., 2005; Shi and Ishizuya-Oka, 1996), which presumably requires extensive changes in gene regulation. Our microarray data reflect this view that many of the changes in gene expression include a significant proportion of transcription factors and development genes. Of all significantly regulated genes involved with transcription, 75% (130 of 169) occur in the second wave of gene expression. Many of these

Table 2
Genes significantly upregulated 1.5× in all tissues: intestine, tail, hind limb, and brain

GenBank	Gene name
DNA replication/Cell Cycle	
AB040073	Ubiquitin activating enzyme
BC054285	CDK2-associated protein 1
Transcription/Translation	
BC041206	cAMP-responsive element-binding protein 1
BC046866	Chromodomain helicase DNA-binding protein 4
BC053765	Chromatin modifying protein 1B
AF351126	Enhancer of zeste
BC048366	Eukaryotic translation initiation factor 4 gamma, 2
AY330768	Arginine methyltransferase 1b
AB085173	Protein arginine methyltransferase 1
BC045260	Heterogeneous nuclear ribonucleoprotein A1
BC043750	Heterogeneous nuclear ribonucleoprotein A2/B1
BC044711	Heterogeneous nuclear ribonucleoprotein K
BC044009	High-mobility group box 3
BC041296	Histone deacetylase 1
BG359854	Putative homeodomain transcription factor 2
AY114105	RAP74 subunit of transcription factor IIF
BC045009	SWI/SNF related, actin-dependent regulator of chromatin
CB197345	WD repeat domain 41
M35362	Thyroid hormone receptor, beta
Z34463	*Xenopus* NFI-X2 transcription factor
BC045237	Translation initiation factor eIF4A II
BC059298	Ribosome-binding protein 1 homolog
BC043623	RNA-binding motif, single-stranded interacting protein 1
Protein metabolism/transport	
BF611398	UDP-glucose ceramide glucosyltransferase-like 1 isoform 2
X54240	p97 subunit of 15S Mg(2+)-ATPase
BU913725	Syntaxin-binding protein 3
AF232672	FK506-binding protein
BC044107	Glutamate-cysteine ligase, modifier subunit
BC056069	Cytosolic non-specific dipeptidase 2
BX853578	Peptidyl-prolyl *cis/trans* isomerase
Z27093	Stromelysin-3
Cell signaling	
BJ074208	Complement component 5
BC042343	Gap junction protein, alpha 7
X75938	Fascin
AY050645	Insulin-like growth factor 2
BC044123	G protein, alpha inhibiting activity polypeptide 3
BC044687	Secreted frizzled-related protein 2
AY458020	Tumor necrosis factor receptor superfamily
BC045134	Tyrosine protein kinase pp60-c-src
Cell structure	
BC043808	Calponin 1
BC046257	Calponin 2
BC046940	Drebrin-like
CA792070	Myosin, heavy polypeptide 4, skeletal muscle
M76710	Cell adhesion molecule
BC054220	Tropomyosin
BC049004	Tubulin, beta 5
AB025246	Coronin homolog, actin-binding protein
Miscellaneous	
BX849102	Prostatic-binding protein
AY277696	Chloride intracellular channel protein 4
BC044315	Lysophospholipase II
L28111	Deiodinase, iodothyronine, type III

Table 2 (continued)

GenBank	Gene name
Unknown function	
U41854	Neuronal protein 3.1
U41855	Neuronal protein 3.1
CB943171	NICHD_XGC_Tad2 *Xenopus laevis* cDNA clone
AW639557	Transcribed locus
BG656590	Transcribed locus
BQ399739	Transcribed locus
BQ733202	Transcribed locus
CA793816	Transcribed locus

genes identified in our microarray are also known to be involved in normal mammalian intestine and intestinal malignancies, including notch (**M22874**) (Es et al., 2005; Fre et al., 2005; Schroder and Achim Gossler, 2002), HES1 (**AW148246**) (Jensen et al., 2000), beta-catenin (**M77013**) (Korinek et al., 1997), and wnt-5A (**M55056**) and frizzled 2 (**AF139165**) (Gregorieff et al., 2005). Another pathway upregulated during this period is TGFβ signaling, including TGFβ ligands themselves, Type I and II receptors, and SMADs (Supplemental Fig. S1). The role of this pathway in intestine development has received less attention than WNT, hedgehog, and Notch signaling pathways (Es et al., 2005; Fre et al., 2005; Kuhnert et al., 2004; Ramalho-Santos et al., 2000; Sancho et al., 2004). The WNT, TGFβ, and sonic hedgehog pathways also have an effect on increasing proliferation corroborated by significant upregulation of c-myc (**X14806**) (He et al., 1998) associated with epithelial stem cells (Giannakis et al., 2006; Ishizuya-Oka et al., 2001b; Stolow and Shi, 1995). Even though 149 genes in the late upregulated cluster were significantly enriched in the development and transcription GO categories, each of the other clusters of genes has about 20 genes in these GO categories (Supplemental Table S4).

Presumably, these signaling pathways mediate expression of genes that rebuild the extracellular matrix following activity of genes involved with proteolysis and apoptosis during the initial wave of gene induction. In the late upregulated cluster of genes (Fig. 6C), there were a significant number of proteins associated with extracellular matrix, such as type 1 collagens (**AB034701**, **BC049287**), type III collagen (**AF170319**), type IV collagen (**AF170340**), and microfibrillar-associated protein 2 (**BC041238**).

Another discovery from the microarray was the identification of strongly downregulated GO categories of genes, namely glucose and fatty acid metabolism and the electron transport chain (Fig. 8). Whereas cell death may be associated with changes in glucose metabolism (Rathmell et al., 2003), decreased electron transport and fatty acid metabolism does not have a histological correlate. Nevertheless, this group of genes makes intuitive sense in light of the documented changes at this point in intestinal remodeling, where energy consumption may not be emphasized in apoptotic tissues. Later time points or natural metamorphosis would be expected to have the expression levels of these genes return to expression levels similar to that of the larva to achieve a functional absorptive organ. For example, during natural metamorphosis, IFABP is

downregulated for remodeling and is expressed again at the end of metamorphosis (Ishizuya-Oka et al., 1997b; Shi and Hayes, 1994) to allow fat absorption in the intestine. The expression of this gene decreased over the course of the T3 treatments here, indicating that final differentiation of absorptive cells had not yet occurred.

It is interesting to note that the GO categories of glucose and fatty acid metabolism and the electron transport chain were also downregulated in the muscle but not in the epithelium or mesenchyme of the tail (Das et al., 2006). Such a finding is consistent with the above interpretation since the tail is made of predominantly muscle, which degenerates, just like the major tissue, the epithelium, in the tadpole intestine. Our interpretation is also supported by the fact that in the limb, these same GO categories were found to be upregulated (Das et al., 2006), as the muscles in the limb undergo growth instead of degeneration. Therefore, it appears that GO categories are correlated with cellular activity rather than cell type.

A well-known, yet less understood, feature of T3-induced metamorphosis is the dramatically different organ-specific responses, from tail resorption, limb growth and development, to intestine remodeling. The basis of these different responses to the same hormone is believed to be due to different cascades of gene regulation specific to each tissue. How a single hormone can result in such varied tissue responses can be addressed by identifying tissue-specific genes upregulated by T3 in brain, hind limb, tail, and intestine. Less than 30% of the genes upregulated in the brain, limb, or tail are also upregulated in the intestine, and even fewer downregulated genes are shared among tissues, possibly due to the fact that detection of downregulation is also dependent upon the mRNA stability of the gene affected. On the other hand, it is worth pointing out that many of the GO categories were found in different organs (Das et al., 2006). This is likely due to several reasons: (1) not all genes are annotated into GO, which is biased toward genes of more common biological significance; (2) a GO category common to different organs can contain many genes specific to different organs; and (3) the percentage of tissue-specific genes in GO categories regulated by T3 within a given time frame may be low, thus such GO categories will not be identified as the significant ones.

The greatest similarity in gene lists is between the degenerating tail and the remodeling intestine (Fig. 9). This similarity can be understood in light of the steps of intestinal remodeling starting from cell death and tissue degeneration through proliferation and differentiation. Our hormone treatments allowed progress through the apoptosis phase to the beginning of proliferation, but not differentiation. Similar processes are occurring in the tail and intestine at the beginning of remodeling, where 100% cells in the tail and the vast majority of cells in the intestine, the larval epithelial cells, are destined to die (Dodd and Dodd, 1976; Shi, 1999; Shi and Ishizuya-Oka, 1996). The early response to T3 in the limb is proliferation. The same early proliferative response is true for the brain, even though, like the intestine, the brain undergoes extensive remodeling. The difference between early responses between brain and intestine is that tissue degeneration is not as extensive in the brain. Therefore, comparison of gene expression data across tissues reflects the similarity in initial morphological response to T3, where the most overlap in gene expression was identified between the intestine and tail.

Another major contribution to understanding the role of thyroid hormone in development is to identify upregulated genes independent of organ. Even though the brain, limb, tail, and intestine are affected by T3 in dramatically different ways, they have a core set of 61 genes upregulated by T3 (Table 2). Interestingly, relatively few downregulated genes are shared across organs compared to genes commonly upregulated. Two insights into organ specificity can be garnered from this comparison. The relatively few downregulated genes may suggest that the mechanism of organ specificity to T3 may reside in the downregulated genes. Second, in contrast to lists of genes upregulated in any one organ, the GO category containing the most number of upregulated genes in common among all four is transcription. This common set of development genes in organs with wildly different responses to T3 suggests that they are direct response genes and that the mechanism underlying varied responses to T3 across organs lies in the organ-specific responses to the direct T3 target genes. However, some direct response genes are known to be tissue-specific, such as sonic hedgehog in the intestinal epithelium and stromelysin-3 in fibroblasts. In light of the fact that the majority of genes regulated by T3 are tissue-specific, yet the most common group of genes regulated by T3 across tissues are genes associated with transcription, it is of considerable interest to determine if these transcription-associated genes are indeed direct T3 response genes with a thyroid hormone response element in the regulatory regions. It is quite likely that a combination of organ-specific T3-regulated early genes, especially downregulated ones, and organ-specific responses to the changes in common T3-regulated genes dictates organ-specific metamorphic changes. Thus, another important area of interest will be to determine the downstream targets of the common early regulated genes.

Acknowledgment

Appendix A. Supplementary data

Supplementary data associated with this article can be found, in the online version, at doi:10.1016/j.ydbio.2006.11.037.

References

Amano, T., Yoshizato, K., 1998. Isolation of genes involved in intestinal remodeling during anuran metamorphosis. Wound Repair Regen. 6, 302–313.

Berry, D.L., Rose, C.S., Remo, B.F., Brown, D.D., 1998a. The expression pattern of thyroid hormone response genes in remodeling tadpole tissues defines distinct growth and resorption gene expression programs. Dev. Biol. 203, 24–35.

Berry, D.L., Schwartzman, R.A., Brown, D.D., 1998b. The expression pattern of thyroid hormone response genes in the tadpole tail identifies multiple resorption programs. Dev. Biol. 203, 12–23.

Buchholz, D.R., Tomita, A., Fu, L., Paul, B.D., Shi, Y.-B., 2004. Transgenic analysis reveals that thyroid hormone receptor is sufficient to mediate the thyroid hormone signal in frog metamorphosis. Mol. Cell. Biol. 24, 9026–9037.

Buckbinder, L., Brown, D.D., 1992. Thyroid hormone-induced gene expression changes in the developing frog limb. J. Biol. Chem. 267, 25786–25791.

Cruz-Reyes, J., Tata, J.R., 1995. Cloning, characterization and expression of two *Xenopus* bcl-2-like cell-survival genes. Gene 158, 171–179.

Dahlquist, K.D., Salomonis, N., Vranizan, K., Lawlor, S.C., Conklin, B.R., 2002. GenMAPP, a new tool for viewing and analyzing microarray data on biological pathways. Nat. Genet. 31, 19–20.

Damjanovski, S., Ishizuya-Oka, A., Shi, Y.B., 1999. Spatial and temporal regulation of collagenases-3, -4, and stromelysin - 3 implicates distinct functions in apoptosis and tissue remodeling during frog metamorphosis. Cell Res. 9, 91–105.

Das, B., Cai, L., Carter, M.G., Piao, Y.-L., Sharov, A.A., Ko, M.S.H., Brown, D.D., 2006. Gene expression changes at metamorphosis induce by thyroid hormone in *Xenopus laevis* tadpoles. Dev. Biol. 291, 342–355.

Denver, R.J., Pavgi, S., Shi, Y.B., 1997. Thyroid hormone-dependent gene expression program for *Xenopus* neural development. J. Biol. Chem. 272, 8179–8888.

Dodd, M.H.I., Dodd, J.M., 1976. The biology of metamorphosis. In: Lofts, B. (Ed.), Physiology of the Amphibia. Academic Press, New York, pp. 467–599.

Doniger, S.W., Salomonis, N., Dahlquist, K.D., Vranizan, K., Lawlor, S.C., Conklin, B.R., 2003. MAPPFinder: using Gene Ontology and GenMAPP to create a global gene-expression profile from microarray data. Genome Biol. 4, R7.

Es, J.H.V., van Gijn, M.E., Riccio, O., van den Born, M., Vooijs, M., Begthel, H., Cozijnsen, M., Robine, S., Winton, D.J., Radtke, F., Clevers, H., 2005. Notch/gamma-secretase inhibition turns proliferative cells in intestine crypts and adenomas into goblet cells. Nature 435, 959–963.

Fre, S., Huyghe, M., Mourikis, P., Robine, S., Louvard, D., Artavanis-Tsakonas, S., 2005. Notch signals control the fate of immature progenitor cells in the intestine. Nature 435, 964–968.

Fu, L., Ishizuya-Oka, A., Buchholz, D.R., Amano, T., Shi, Y.-B., 2005. A causative role of stromelysin-3 in ECM remodeling and epithelial apoptosis during intestinal metamorphosis in *Xenopus laevis*. J. Biol. Chem. 280, 27856–27865.

Giannakis, M., Stappenbeck, T.S., Mills, J.C., Leip, D.G., Lovett, M., Clifton, S.W., Ippolito, J.E., Glasscock, J.I., Arumugam, M., Brent, M.R., Gordon, J.I., 2006. Molecular properties of adult mouse gastric and intestinal epithelial progenitors in their niches. J. Biol. Chem. 281, 11292–11300.

Gregorieff, A., Pinto, D., Begthel, H., Destree, O., Kielman, M., Clevers, H., 2005. Expression pattern of Wnt signaling components in the adult intestine. Gastroenterology 129, 626–638.

He, T.C., Sparks, A.B., Rago, C., Hermeking, H., Zawel, L., da Costa, L.T., Morin, P.J., Vogelstein, B., Kinzler, K.W., 1998. Udebtufucatuib if c0NTC as a target of the APC pathway. Science 281, 1509–1512.

Helbing, C.C., Werry, K., Crump, D., Domanski, D., Veldhoen, N., Bailey, C.M., 2003. Expression profiles of novel thyroid hormone-responsive genes and proteins in the tail of *Xenopus laevis* tadpoles undergoing precocious metamorphosis. Mol. Endocrinol. 17, 1395–1409.

Ishizuya-Oka, A., Shimozawa, A., 1991. Induction of metamorphosis by thyroid hormone in anuran small intestine cultured organotypically in vitro. In Vitro Cell. Dev. Biol. 27A, 853–857.

Ishizuya-Oka, A., Ueda, S., 1996. Apoptosis and cell proliferation in the *Xenopus* small intestine during metamorphosis. Cell Tissue Res. 286, 467–476.

Ishizuya-Oka, A., Stolow, M.A., Ueda, S., Shi, Y.B., 1997a. Temporal and spatial expression of an intestinal Na$^+$/PO$_4$ 3- cotransporter correlates with epithelial transformation during thyroid hormone-dependent frog metamorphosis. Dev. Genet. 20, 53–66.

Ishizuya-Oka, A., Ueda, S., Damjanovski, S., Li, Q., Liang, V.C., Shi, Y.-B., 1997b. Anteroposterior gradient of epithelial transformation during amphibian intestinal remodeling: immunohistochemical detection of intestinal fatty acid-binding protein. Dev. Biol. 192, 149–161.

Ishizuya-Oka, A., Li, Q., Amano, T., Damjanovski, S., Ueda, S., Shi, Y.-B., 2000. Requirement for matrix metalloproteinase stromelysin-3 in cell migration and apoptosis during tissue remodeling in *Xenopus laevis*. J. Cell Biol. 150, 1177–1188.

Ishizuya-Oka, A., Ueda, S., Amano, T., Shimizu, K., Suzuki, K., Ueno, N., Yoshizato, K., 2001a. Thyroid-hormone-dependent and fibroblast-specific expression of BMP-4 correlates with adult epithelial development during amphibian intestinal remodeling. Cell Tissue Res. 303, 187–195.

Ishizuya-Oka, A., Ueda, S., Inokuchi, T., Amano, T., Damjanovski, S., Stolow, M., Shi, Y.-B., 2001b. Thyroid hormone-induced expression of Sonic hedgehog correlates with adult epithelial development during remodeling of the *Xenopus* stomach and intestine. Differentiation 69, 27–37.

Jensen, J., Pedersen, E.E., Galante, P., ald, J., Heller, R.S., Ishibashi, M., Kageyama, R., Guillemot, F., Serup, P., Madsen, O.D., 2000. Control of endodermal endocrine development by Hes-1. Nat. Genet. 24, 36–44.

Korinek, V., Barker, N., Morin, P.J., van Wichen, D., de Weger, R., Kinzler, K.W., Vogelstein, B., Clevers, H., 1997. Constitutive transcriptional activation by a b-catenin-Tcf complex in APC$-/-$ colon carcinoma. Science 275, 1784–1787.

Kuhnert, F., Davis, C.R., Wang, H.-T., Chu, P., Lee, M., Yuan, J., Nusse, R., Kuo, C.J., 2004. Essential requirement for Wnt signaling in proliferation of adult small intestine and colon revealed by adenoviral expression of Dickkopf-1. Proc. Natl. Acad. Sci. 101, 266–271.

McAvoy, J.W., Dixon, K.E., 1977. Cell proliferation and renewal in the small intestinal epithelium of metamorphosing and adult *Xenopus laevis*. J. Exp. Zool. 202, 129–138.

Nakajima, K., Takahashi, A., Yaoita, Y., 2000. Structure, expression, and function of the *Xenopus laevis* caspase family. J. Biol. Chem. 275, 10484–10491.

Nieuwkoop, P.D., Faber, J., 1956. Normal Table of *Xenopus laevis*. North Holland Publishing, Amsterdam.

Pasquier, D.D., Rincheval, V., Sinzelle, L., Chesneau, A., Ballagny, C., Sachs, L.M., Demeneix, B., Mazabraud, A., 2006. Developmental cell death during *Xenopus* metamorphosis involves BID cleavage and caspase 2 and 8 activation. Dev. Dyn. 235, 2083–2094.

Patterton, D., Hayes, W.P., Shi, Y.B., 1995. Transcriptional activation of the matrix metalloproteinase gene stromelysin-3 coincides with thyroid hormone-induced cell death during frog metamorphosis. Dev. Biol. 167, 252–262.

Ramalho-Santos, M., Melton, D.A., McMahon, A.P., 2000. Hedgehog signals regulate multiple aspects of gastrointestinal development. Development 127, 2763–2772.

Ranjan, M., Wong, J., Shi, Y.B., 1994. Transcriptional repression of *Xenopus* TR beta gene is mediated by a thyroid hormone response element located near the start site. J. Biol. Chem. 269, 24699–24705.

Rathmell, J.C., Fox, C.J., Plas, D.R., Hammerman, P.S., Cinalli, R.M., Thompson, C.B., 2003. Akt-directed glucose metabolism can prevent Bax conformation change and promote growth factor-independent survival. Mol. Cell. Biol. 23, 7315–7328.

Rowe, I., Le Blay, K., Pasquier, D.D., Palmier, K., Levi, G., Demeneix, B., Laurent Coen, L., 2005. Apoptosis of tail muscle during amphibian metamorphosis involves a caspase 9 dependent mechanism. Dev. Dyn. 233, 76–87.

Sachs, L.M., Le Mevel, B., Demeneix, B.A., 2004. Implication of bax in *Xenopus laevis* tail regression at metamorphosis. Dev. Dyn. 231, 671–682.

Sancho, E., Batlle, E., Clevers, H., 2004. Signaling pathways in intestinal development and cancer. Annu. Rev. Cell Dev. Biol. 20, 695–723.

Schreiber, A.M., Cai, L., Brown, D.D., 2005. Remodeling of the intestine during metamorphosis of *Xenopus laevis*. Proc. Natl. Acad. Sci. U. S. A. 102, 3720–3725.

Schroder, N., Achim Gossler, A., 2002. Expression of notch pathway components in fetal and adult mouse small intestine. Gene Expr. Patterns 2, 247–250.

Shi, Y.-B., 1999. Amphibian Metamorphosis: From Morphology to Molecular Biology. John Wiley & Sons, Inc., New York.

Shi, Y.-B., Brown, D.D., 1993. The earliest changes in gene expression in tadpole intestine induced by thyroid hormone. J. Biol. Chem. 268, 20312–20317.

Shi, Y.-B., Hayes, W.P., 1994. Thyroid hormone-dependent regulation of the intestinal fatty acid-binding protein gene during amphibian metamorphosis. Dev. Biol. 161, 48–58.

Shi, Y.-B., Ishizuya-Oka, A., 1996. Biphasic intestinal development in

amphibians: embryogenesis and remodeling during metamorphosis. Curr. Top. Dev. Biol. 32, 205–235.

Shi, Y.B., Ishizuya-Oka, A., 1997. Autoactivation of *Xenopus* thyroid hormone receptor beta genes correlates with larval epithelial apoptosis and adult cell proliferation. J. Biomed. Sci. 4, 9–18.

Stolow, M.A., Shi, Y.B., 1995. *Xenopus* sonic hedgehog as a potential morphogen during embryogenesis and thyroid hormone-dependent metamorphosis. Nucleic Acids Res. 23, 2555–2562.

Stolow, M.A., Bauzon, D.D., Li, J., Sedgwick, T., Liang, V.C., Sang, Q.A., Shi, Y.B., 1996. Identification and characterization of a novel collagenase in *Xenopus laevis*: possible roles during frog development. Mol. Biol. Cell 7, 1471–1483.

Tata, J.R., 1993. Gene expression during metamorphosis: an ideal model for post-embryonic development. BioEssays 15, 239–248.

Wang, Z., Brown, D.D., 1993. Thyroid hormone-induced gene expression program for amphibian tail resorption. J. Biol. Chem. 268, 16270–16278.

Yaoita, Y., Nakajima, K., 1997. Induction of apoptosis and CPP32 expression by thyroid hormone in a myoblastic cell line derived from tadpole tail. J. Biol. Chem. 272, 5122–5127.

Zeeberg, B.R., Feng, W., Wang, G., Wang, M.D., Fojo, A.T., Sunshine, M., Narasimhan, S., Kane, D.W., Reinhold, W.C., Lababidi, S., Bussey, K.J., Riss, J., Barrett, J.C., Weinstein, J.N., 2003. GoMiner: a resource for biological interpretation of genomic and proteomic data. Genome Biol. 4, R28.